Variable geometry gas turbines for improving the part-load performance of marine combined cycles - Combined cycle performance

F. Haglind

Accepted Manuscript

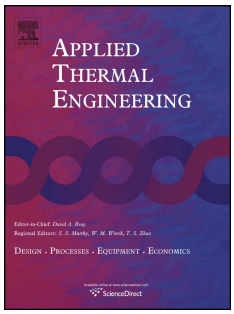

Title: Variable geometry gas turbines for improving the part-load performance of marine combined cycles – Combined cycle performance

Authors: F. Haglind

PII: S1359-4311(10)00425-4

DOI: 10.1016/j.applthermaleng.2010.09.029

Reference: ATE 3256

To appear in: *Applied Thermal Engineering*

Received Date: 15 February 2010

Revised Date: 28 September 2010

Accepted Date: 29 September 2010

Please cite this article as: F. Haglind. Variable geometry gas turbines for improving the part-load performance of marine combined cycles – Combined cycle performance, Applied Thermal Engineering (2010), doi: 10.1016/j.applthermaleng.2010.09.029

Variable geometry gas turbines for improving the part-load performance of marine combined cycles – Combined cycle performance

F. Haglind*

Technical University of Denmark, Department of Mechanical Engineering, DK-2800 Kgs. Lyngby, Denmark

ABSTRACT

The part-load performance of combined cycles intended for naval use is of great importance, and it is influenced by the gas turbine configuration and load control strategy. This paper is aimed at quantifying the effects of variable geometry gas turbines on the part-load efficiency for combined cycles used for ship propulsion. Moreover, the paper is aimed at developing methodologies and deriving models for part-load simulations suitable for energy system analysis of various components within combined cycle power plants. Two different gas turbine configurations are studied, a two-shaft aero-derivative configuration and a single-shaft industrial configuration. The results suggest that by the use of variable geometry gas turbines, the combined cycle part-load performance can be improved. In order to minimise the voyage fuel consumption, a combined cycle featuring two-shaft gas turbines with

* Corresponding author. Tel.: +45 45 25 41 13; fax: +45 45 93 52 15.
E-mail address: frh@mek.dtu.dk (F. Haglind)

VAN control is a promising alternative for container ships, while a cycle with single-shaft gas turbine configurations with VGV control is indicated to be an equally good choice for tankers and carriers.

Keywords: Variable geometry; Gas turbine; Combined cycle; Part-load; Performance; Marine applications

Nomenclature

Abbreviations and chemical formulae

DNA Dynamic Network Analysis (computer simulation program)

DWT deadweight tonnage (total carrying capacity of a ship in 1000 kg)

HRSG heat recovery steam generator

MCR maximum continues rating

MGO marine gas oil

SCR service continues rating

SO_2 sulphur dioxide

SO_3 sulphur trioxide

TEU twenty-foot equivalent unit

VAN variable area nozzle

VGV variable guide vane

Notations

A Area (m^2)

C_T turbine constant (kg $K^{1/2}$/s bar)

LHV lower heating value (MJ/kg)

LMTD logarithmic mean temperature difference (K)

P pressure (bar)

Pr Prandtl number

Q heat transfer (kW)

T temperature (K)

U overall heat transfer coefficient (kW/m^2 K)

W mass flow (kg/s)

ΔT temperature difference at heat exchanger end (K)

α heat transfer coefficient (kW/m^2 K)

ε effectiveness

η efficiency

η_0 surface efficiency

η_f fin efficiency

λ thermal conductivity (W/m K)

μ viscosity (kg/m s)

Subscripts

1 steam turbine inlet

2 steam turbine outlet

CC combined cycle

D design

f fin

g gas

GT gas turbine

w water/steam

1. Introduction

Today the great majority of prime movers and auxiliary plants of ocean-going ships are diesel engines. In terms of maximum installed engine power of all civilian ships above 100 gross tons, 96% is produced by diesel engines [1]. As for large ships, almost all are powered by slow-speed, two-stroke diesel engines. The primary reasons for this dominance are their high efficiency (also at part-load), and that they can run on heavy fuel oil (residual fuel oil manufactured at the “bottom end” of the oil refining process).

A combined cycle featuring one or several gas turbines and a steam cycle is a power plant option commonly used for power production that offers high efficiency. Combined cycles have rarely been used in the past for propulsion of ships, but following the expected legislative actions, increasing environmental awareness and the increasing price of heavy fuel oil, it might be a viable option for the future [2-4]. The primary advantages of using gas and steam turbine combined cycles for propulsion of large ships include lower weight and space requirement for the prime mover system, as well as lower amounts of pollutant emissions. These issues are discussed in Haglind [3] and Haglind [4].

Because of the considerable portion of the running time spent at part power, the part-load performance of combined cycles intended for naval use is of great importance. Then, the question arises which gas turbine configuration and which control strategy maximise the plant efficiency of a combined cycle in part-load. If the fuel mass flow

is neglected, i.e. it is assumed that the heat is added to the gas turbine cycle in a heat exchanger, and the combustion efficiency is assumed to be 100%, the following expression for the net plant efficiency for a combined cycle can be derived:

$$\eta_{CC} = \eta_{GT} + (1 - \eta_{GT})\,\varepsilon_{HRSG}\,\eta_{Rankine} \quad (1)$$

where η_{GT} is the gas turbine efficiency, ε_{HRSG} is the effectiveness of the heat recovery steam generator (HRSG) (i.e. the ratio of heat transferred in the HRSG to heat transferrable in the HRSG), and $\eta_{Rankine}$ is the efficiency of the steam cycle (i.e. the ratio of net power output of the steam cycle to heat transferred in the HRSG). The heat transferrable in the HRSG is defined as the amount of heat that would be transferred if the stack temperature was equal to the ambient temperature.

The effectiveness of the HRSG is influenced primarily by the steam cycle design, e.g. number of pressure levels, stack temperature and pinch-points within the HRSG. In part-load, the ε_{HRSG} is affected by the properties (primarily mass flow) of the gas turbine exhaust flow, because of their effects on the heat transfer coefficients within the HRSG and hence also on pinch-points. Depending on the gas turbine configuration and load control strategy, the mass flow, temperature and composition of the gas turbine exhaust flow vary in part-load. That is, the gas turbine part-load behaviour affects the ε_{HRSG}. Furthermore, the gas turbine configuration and load control strategy influence the exhaust temperature, and thus, the mean temperature of the heat supply for the steam cycle, which affects the efficiency of the steam cycle.

The approach adapted here is to maintain the gas turbine exhaust temperature to the extent possible in part-load using variable area, thereby maintaining the heat recovery capability, with as small as possible decrease in efficiency for the gas turbine. There are primarily two ways of changing the gas turbine geometry for controlling the load: compressor variable guide vanes (VGVs) and turbine variable area nozzle (VAN).

The use of VGVs as a means of improving the part-load performance for stationary combined cycles has been addressed previously [5-10]. In fact, in fairly modern stationary combined cycles, the gas turbine(s) is generally equipped with three rows of VGVs, allowing a high gas turbine exhaust gas temperature down to 40% load [11]. As far as recuperated gas turbines are concerned, it is common practice to use a power turbine with VAN [12]. The advantages of VAN load control over pure fuel load control for recuperated gas turbines have been demonstrated in studies [e.g. 13] and by practical experience for the marine gas turbine WR-21 [14]. More information about the WR-21 engine can be found in references 15-20. For combined cycles there also might be a potential for improving the part-load performance by employing a variable area turbine, which has not previously been thoroughly evaluated. Moreover, previous studies on part-load performance of combined cycles were focused on stationary applications, for which full load operating conditions and slightly below are of primary interest. In contrast, also lower load conditions are of importance when considering plants to be used for marine propulsion. The use of VGVs and/or VAN has also been suggested for achieving higher part-load efficiencies for gas turbines [21-24].

This paper is aimed at quantifying the effects of variable geometry gas turbines on the part-load efficiency for combined cycles used for ship propulsion. Moreover, the paper is aimed at developing methodologies and deriving models for part-load simulations suitable for energy system analysis of various components within combined cycle power plants. In contrast to many of the previous works within this field, in this work the part-load characteristics of all components within combined cycles are considered, including those of generators and gears. Two different gas turbine configurations are studied, a two-shaft aero-derivative configuration and a single-shaft industrial configuration. As for the two-shaft configuration, the load is controlled by fuel flow and a VAN, respectively. The load of the single-shaft arrangement is controlled by fuel flow and compressor VGVs, respectively. Gas turbine as well as combined cycle performances are obtained over the load range, covering 40-100% (for the combined cycle), which is the range in which large ships normally are operated at sea. Moreover, the combined cycles are evaluated with respect to ship voyage performances.

It is worth mentioning that no attempt is made in this study to design combined cycles that attain the highest achievable performance. For instance, by using a reheat gas turbine [25] and a more advanced steam cycle including reheat and more pressure levels [26], it would be possible to achieve higher efficiency figures than those reported here. The formation of pollutant emissions is not addressed. It is possible that the inclusion of technologies for reducing emissions would affect the way the gas turbine is controlled in part-load, making it suitable to revise the load control methods studied here.

Considering large ship types like container vessels, bulk carriers and tankers, it is the container vessel that requires the greatest propulsion powers. In terms of load capacity, the majority of container ship orders today are in the Post-Panamax (i.e. not able to pass the Panama Canal) and New Panamax (i.e. able to pass the Panama Canal after a widening) classes, carrying in the range of 5 101-14 500 twenty-foot equivalent unit (TEU) containers [27]. The largest vessels currently delivered can carry 15 500 TEU, which corresponds to a propulsion power demand of about 76 MW. In the future, ultra large vessels carrying up to 22 000 TEU are expected, requiring a propulsion power of about 90 MW.

While container ships have an average speed in service of up to 25 knots, bulk carriers and tankers are sailing at speeds of about 15 knots or less [28,29]. The propulsion power needed is proportional to the ship speed to approximately the fourth power, and consequently, the propulsion power requirements of bulk carriers and tankers are less than those of container vessels. The largest bulk carriers (carrying about 320 000 DWT) require a propulsion power of about 25 MW [28], and the largest crude carriers (tankers) (carrying about 560 000 DWT) require about 40-45 MW for propulsion [29]. In this work, for meeting the power requirements of future large container vessels while having operational flexibility, combined cycles consisting of two gas turbines (of the size of the LM2500+) with heat recovery steam generators (HRSGs) and one steam cycle are considered.

Due to the increasing pressure on ship owners to reduce fuel consumption and pollutant emissions, natural gas-fired gas and steam turbine combined cycles may also be an option for high-speed ferries. Today these vessels are powered either by diesel-

fuelled piston engines or gas turbines. The propulsion power demand for such vessels is large; the largest ferries in operation today require a minimum of 36 MW at 38 knots, while vessels available within the next 5-10 years are expected to require about 45-50 MW at 38 knots (D. Nielsen, Mols-Linien, Aarhus, Denmark, 2009, private communication). Moreover, to be suitable for high-speed ferries, the propulsion system needs to be light and compact.

When using combined cycle power plants for ships, either the turbines can directly drive propeller shafts or a turbo-electric transmission can be used [2]. Turbo-electric transmission implies that electric generators convert the mechanical energy of the turbines (steam and/or gas) into electric energy, and an electric motor powers the propeller shaft. In this work, combined cycles with the gas and steam turbines connected to generators rotating with constant speeds are considered.

In this paper, the modelling approach and derivation of the models are described in Section 2. The design of the steam cycle is outlined in Section 3. Combined cycle performances versus load are presented in Section 4, and in Section 5 each of the combined cycles are evaluated with respect to average efficiencies for ship voyages. Finally, in Section 5 the conclusions are outlined and discussed.

2. Modelling

In this section the modelling tool used for the simulations is described, and the derivations of models are outlined for part-load simulation suitable for energy system analysis of various components within combined cycles. The modelling details related to the gas turbine, namely, variable geometry, pressure loss, gear and generator, are

described in Haglind [30], while this section is focused on the modelling details of components within the steam cycle.

2.1. DNA – the performance modelling tool

The results reported within the paper are obtained using the simulation program DNA (Dynamic Network Analysis), which is a program used for energy systems analyses [31-33]. DNA is the present result of an ongoing development at Technical University of Denmark, Department of Mechanical Engineering. The compressor and turbines in this paper are modelled using component maps, and variable geometry is modelled by correcting the data read in the maps, as explained in Haglind [30]. More information about component maps and detailed descriptions about the use of maps in DNA are given in Haglind and Elmegaard [34]. Furthermore, in Haglind and Elmegaard [34] is included a validation of the DNA model used here for estimating design point and part-load performances of gas turbines. The validity of simulating other components within combined cycles in DNA is demonstrated in, for instance, Elmegaard [32].

2.1. Heat recovery steam generator

The combined cycle considered consists of a number of heat exchangers, for which the performance in part-load is changed. It is common practice to formulate the overall duty of a heat exchanger as:

$$Q = U\,A\,\mathrm{LMTD} \tag{2}$$

where U is the overall heat transfer coefficient, A is the heat transferring area, and LMTD is the logarithmic mean temperature difference. In this work, heat exchangers

are assumed to be of pure counter-current configurations, for which LMTD is given by:

$$\mathrm{LMTD} = \frac{\Delta T_g - \Delta T_w}{\ln\left(\frac{\Delta T_g}{\Delta T_w}\right)} \tag{3}$$

where ΔT_g and ΔT_w are the temperature differences at the gas and water/steam ends of the heat exchanger, respectively.

It is recognised that the thermal resistance of tube walls are relatively negligible, and hence the overall heat transfer coefficient on the gas side can be written as:

$$U_g = \frac{\alpha_g}{\frac{1}{\eta_0} + \frac{\alpha_g A_g}{\alpha_w A_w}} \tag{4}$$

where α denotes the heat transfer coefficient, η_0 denotes the surface efficiency, and the indexes g and w refer to the gas and the water/steam side, respectively. The surface efficiency is included to take account for a decreased temperature effectiveness of fins on the gas side.

With respect to part-load performance, different methodologies are applied for the economiser and evaporator, and the superheater. In the economiser and the evaporator, the heat transfer on the gas side is 10-100 times smaller than that on the water/steam side [35], i.e. the gas side thermal resistance controls the heat transfer.

That is, the ratio of the overall heat transfer coefficient in a certain operating point to that in design can be written as (any variation of surface efficiency with load is neglected):

$$\frac{U_g}{U_{g,D}} = \frac{\alpha_g}{\alpha_{g,D}} \tag{5}$$

Using Nusselt correlations, the ratio of heat transfer coefficients (at any side) can be expressed as:

$$\frac{\alpha}{\alpha_D} = \left(\frac{W}{W_D}\right)^m \left(\frac{\mu_D}{\mu}\right)^m \left(\frac{\mathrm{Pr}}{\mathrm{Pr}_D}\right)^n \left(\frac{\lambda}{\lambda_D}\right) \tag{6}$$

where μ denotes viscosity, Pr denotes Prandtl number, and λ denotes thermal conductivity. The physical properties can be assumed constant with reasonably good accuracy [35], and thus it follows from Eqs. (5) and (6) that the ratio of gas-side heat transfer coefficients in the economiser and evaporator can be expressed as:

$$\frac{U_g}{U_{g,D}} = \left(\frac{W_g}{W_{g,D}}\right)^m \tag{7}$$

Typical values for the exponent *m* are 0.56-0.58 for staggered tubes and 0.59-0.65 for in-line tubes [35]. In this work, the product U_g times A_g for the economiser and evaporators is determined in design (for attaining a desired pinch-/approach point),

and in off-design this product is corrected using Eq. (7) (A_g is constant), assuming m equal to 0.58.

In the superheater, however, the thermal resistance on the steam side should not be neglected. Here, the overall heat transfer coefficient is computed using Eq. (4). In design, reasonable values for α_g and $\alpha_g A_g/\alpha_w A_w$ are assumed, namely, 0.08 kW/m^2 K and 0.667 [7]. A surface efficiency of 0.8 is computed with the following formula, using reasonable assumptions for fin efficiency (~0.7) and ratio of fin area to total area (~0.7): $\eta_0=1-A_f/A*(1-\eta_f)$ [36]. The surface efficiency is assumed not to vary with load. With these assumptions, an overall heat transfer coefficient of 0.042 kW/m^2 K is obtained for the superheater, which agrees very well with figures reported in De Salva et al. [37] for comparable superheaters. Having calculated U_g in design, the gas-side heat transferring area can be derived.

In part-load, $\alpha_g A_g/\alpha_w A_w$ needs to be re-calculated. The ratios of heat transfer coefficients on the gas and water/steam side, respectively, are calculated using Eq. (6), with physical properties assumed constant. Since the flow characteristics are different on the steam side compared to those on the gas side (i.e. flow inside tubes instead of across an array of tubes), the exponent m is given the value 0.8 [7] when considering the steam side. Subsequently, $\alpha_g A_g/\alpha_w A_w$ is computed with the following equation:

$$\frac{\alpha_g A_g}{\alpha_w A_w} = \frac{\alpha_g / \alpha_{g,D}}{\alpha_w / \alpha_{w,D}} \left(\frac{\alpha_g A_g}{\alpha_w A_w} \right)_D \tag{8}$$

Pressure losses within the heat exchangers in part-load are estimated by neglecting effects of the Reynolds number and hence considering the pressure loss proportional to fluid density times the fluid velocity squared (see Haglind [30]).

2.2. Steam turbine

In this work, the steam turbine flow characteristics in part-load are governed by a turbine constant (or the flow coefficient), i.e. a constant that governs the relation between flow and operating condition for the turbine. Using Stodola's ellipse and assuming ideal gas, the following expression for the turbine constant may be derived [34,38,39]:

$$C_T = \frac{W_1 \sqrt{T_1}}{\sqrt{P_1^2 - P_2^2}} \tag{9}$$

where W is the mass flow, T is the temperature and P is the pressure. The subscripts 1 and 2 refer to the turbine inlet and outlet, respectively. What remains possibly to consider are steam turbine losses and variations with load of the isentropic efficiency.

The performance of a steam turbine at design flow is governed by [40]:

- Expansion line efficiency, which is determined for each section by
    - Volume flow
    - Pressure ratio
    - Initial pressure and temperature
    - Governing stage design (if any)
- Exhaust loss

- Packing and valve steam leakage flows
- Mechanical losses
- Generator losses

For part-load conditions, the efficiency of stages between the first stage and a few stages preceding the last stage is the same as at design. If the turbine features a governing stage, the efficiency for this stage will be affected in part-load; how much, is determined by the throttle flow. The efficiency of the last stages is affected by an exhaust loss, which is primarily a function of the annulus velocity of the last stage. The major component of the total exhaust loss is the leaving loss. Furthermore, the condensing section of the turbine is affected by a moisture loss. From saturation down to the Wilson line (located at the point where the condensation starts, which is at a steam quality of about 0.97) there is a supersaturation loss, and beyond that point there is a moisture loss with no supersaturation loss [41].

The exhaust loss characteristic is a unique feature of each low-pressure turbine, and it used to be presented by the manufacturers as specific enthalpy loss versus annulus steam velocity. In the procedure of calculating the exhaust loss, correction is made also for the moisture content of the flow. Typical exhaust loss figures at design are 20-50 kJ/kg s (J. Nyqvist, Siemens Industrial Turbomachinery, Finnspång, Sweden, 2007, private communication).

Losses owing to packing and valve steam leakage flows are not believed to play any significant role for the part-load performance. That is, modelling them separately or including them when selecting a figure for the isentropic efficiency makes no

significant difference. The losses that may change in part-load include the gear loss (small-size steam turbines generally include a gear to maximise the efficiency of the steam turbine), the mechanical loss, the exhaust loss and the generator loss. However, for the limited load range considered here for the steam turbine, namely about 50-100%, their variations with load are expected to be fairly small. The influence of exhaust loss is estimated by computing the steam turbine output at about 45% combined cycle load, both considering the exhaust loss following the methodology outlined in Spencer et al. [40] and not considering the exhaust loss. The result indicates that the difference in power output is in the order of 100 kW, which corresponds to less than 0.3% of the combined cycle output.

The performances of the steam turbine modelled in this work are adjusted to match those of the Siemens steam turbine SST-300. This turbine is selected because of its suitability for combined cycle applications, and because its size and turbine inlet conditions match those of the steam turbine modelled in this work. Aligning the model to the performances of the SST-300 steam turbine is therefore expected to provide reasonable model assumptions. For the time being, this machine is not particularly adopted for marine applications. However, the adoptions required for marine applications are related to practical installation issues and not to the performance of the machine.

As the combined cycle is operated in sliding pressure mode over the whole operating regime considered here (see Section 4), any governing stage is not considered. A comparison with the part-load performance of the SST-300 suggests that it would be possible to attain fairly good agreement with a simple model, not considering all the

variations with load of all individual losses. The approach adapted is to estimate the flow characteristics using the turbine constant (Eq. (9)) and only including the influence of generator efficiency following the methodology outlined in Haglind [30]. That is, all other losses are included when selecting an isentropic efficiency at design. In part-load the isentropic efficiency is kept constant. Based on these assumptions, the isentropic efficiency should be 0.87 to match power output of the SST-300 machine (J. Nyqvist, Siemens Industrial Turbomachinery, Finnspång, Sweden, 2007, private communication). With respect to part-load performances, good agreement with those of the SST-300 steam turbine is achieved.

3. Combined cycle design

As outlined in Section 1, combined cycles consisting of two gas turbines with HRSGs and one steam cycle are considered. For reasons discussed in Haglind 2008 [2], a drum-type HRSG with vertical gas flow mounted directly over the gas turbine is suggested to be a viable option for marine applications. The steam cycle consists of two pressure levels, with only an evaporator included on the low-pressure side, placed at the end of the HRSG. The main purpose of introducing this low-pressure evaporator is to maintain the stack temperature in part-load (see Section 4). A schematic picture of the combined cycle is shown in Fig. 1 (for simplicity, only one gas turbine with HRSG is shown). The simulations are conducted with a light distillate fuel with a lower heating value (LHV) of 42.798 MJ/kg, with a fuel composition typical for Marine Gas Oil (MGO). Ambient conditions are assumed to be 15 °C and 1.01325 bar.

3.1. Gas turbine design

The design of the gas turbines is outlined in detail in Haglind [30]; here only a brief summary is given. The gas turbine selected to form the basis for this study is LM2500+ manufactured by General Electric. It is an aero-derivative gas turbine with the gas generator mechanically uncoupled from the power turbine. Based on performance data for design condition for the LM2500+ gas turbine provided by General Electric, a performance model is created in DNA. Turbine cooling and pressure losses are modelled. The single-shaft configuration is obtained by removing the power turbine connecting the gas generator to the generator through a gear. The isentropic efficiency for the turbine is adjusted to get the same polytrophic efficiency as those of the turbines of the two-shaft configuration (which are about the same). The cooling flow distribution is changed to obtain the same power output as the two-shaft configuration if the gear loss is disregarded. Exhaust temperature and power output of the gas turbines when combined with the steam cycles are given in Table 2.

3.2. Steam cycle design

The design of the HRSG is a compromise between plant performance, and costs and space requirement. Costs are driven primarily by the heat exchanger surface installed, which in turn, is affected mainly by the pinch-point in the evaporator. While the surface of the evaporator increases exponentially as the pinch-point decreases, the increase in amount of steam generated is only linear [11]. For installations where efficiency is highly valued, Kehlhofer et al. [11] suggest a pinch-point of 8-15 ºC, and where efficiency is of lesser value, a higher range is suggested, 15-25 ºC. In this work, pinch-points of 10 ºC are used in the evaporators.

During off-design conditions, steam can be generated in the economiser, which may block tubes and reduce the performance of the HRSG. Therefore, economisers are dimensioned so that the feedwater at the outlet is slightly sub-cooled at full load. This sub-cooling, often called the economiser approach (i.e. the difference between the saturation temperature and the water temperature at the economiser outlet), causes, for a given design, a reduction in the amount of steam generated, and should therefore be kept as small as possible. Kehlhofer et al. [11] suggest a value in the range of 5-12 ºC. In this work, different economiser approaches are adapted for the different load control methods in order to avoid steaming in the economisers in part-load. For fuel flow control, 60 ºC is used for the cycle based on the single-shaft gas turbine and 100 ºC for the cycle based on the two-shaft gas turbine. As for the variable area control methods, the corresponding figures are 20 ºC and 5 ºC for the cycles based on single and two-shaft gas turbines, respectively. As modelled here, selecting different figures for the economiser approaches does not affect the performance, because that only affects the division of heat duty between the economiser and evaporator which, in turn, affects their area requirements.

Another parameter in the HRSG influencing the performance and area requirement of the HRSG is the superheater approach, i.e. the temperature difference between the gas turbine exhaust and the superheated steam out of the HRSG. Here a superheater approach of 30 ºC is used. Also the pressure drops on the gas side and water/steam side affect the HRSG performance. On the one hand, the pressure drop on the gas side should be low in order to limit losses in power output and efficiency of the gas turbine. On the other hand, in order to obtain a good rate of heat recovery in the HRSG, large surfaces are required, which causes large pressure drops. The pressure

drops on the water/steam side affect only the pump works and play a minor role for the combined cycle performance. Reasonable pressure drops on the gas side of modern HRSGs are in the range of 25-37 mbar [11,42]. In this work, a pressure drop of 30 mbar on the gas side and 6.67 bar on the water/steam side (which is 10% of the maximum steam pressure) for the whole HRSG are assumed.

The selection of condenser pressure will have an effect on the overall plant performance. The lower the condenser pressure, the higher the overall efficiency. However, in practice the minimum condenser pressure is limited by the temperature of the cooling water available and by the minimum acceptable steam quality at the low-pressure end. For the computations conducted here, a sea water temperature of 12 ºC is assumed. Assuming a cooling water temperature difference of 10 ºC, the cooling water is heated to 22 ºC. In a condenser the heat transfer is extremely efficient; hence, only a few degrees' difference between the saturation temperature of the steam and the temperature of the cooling water out of the condenser is sufficient. Here, a condenser pressure of 0.035 bar is selected, corresponding to a saturation temperature of 26.5 ºC. Accordingly, there is 4.5 ºC marginal to the saturation temperature. When the ship is sailing in tropical waters, the condenser pressure needs to be increased, which will have a detrimental effect on the plant performance. And vice versa, when the ship is sailing in winter conditions with a sea water temperature close to zero, the condenser pressure can be reduced, resulting in improved plant efficiency.

Part of the sulphur dioxide (SO_2) produced when burning a sulphur-bearing fuel is converted to sulphur trioxide (SO_3), which combines with moisture to form sulphuric

acid vapour [42]. This vapour condenses on surfaces below its dewpoint of about 120-150 ºC, and may thus cause acid dewpoint corrosion at the HRSG end. By keeping the metal temperature, which is primarily governed by the feedwater temperature, above this temperature, corrosion can be avoided. However, it would result in a low HRSG effectiveness. Generally, HRSGs are designed to operate at minimum metal temperatures somewhat below the acid dewpoint, where the efficiency gained more than balances the additional maintenance costs [42]. For plants burning distillate oil with a maximum fuel sulphur content of 1 $\%_{mass}$, Stultz and Kitto [42] recommend a minimum metal temperature of 104 ºC. In this work the feedwater is pre-heated in the feedwater tank to 104 ºC using steam produced in the low-pressure evaporator. The steam produced in the low-pressure evaporator not needed for feedwater pre-heating, is expanded in the steam turbine. For the conditions simulated here, at design about half of this steam is needed for feedwater pre-heating and half is used to generate additional power.

Having defined the gas turbine (and thereby its exhaust temperature) and the superheater approach, it follows that the live steam temperature is 506.8 ºC. In order not to sacrifice the performance of the last stages of the low-pressure turbine, the steam quality at the low-pressure end needs to be kept above a certain minimum level. Following the recommendations from steam turbine manufacturers, such a limiting value is commonly within the range of 0.86-0.89 [43]. Selecting a live steam pressure of 60 bar results in a steam quality of 0.867, which is considered acceptable. Pumps and the generator are given efficiency figures representative for state-of-the-art. The background for the selected isentropic efficiency for the steam turbine is outlined in Section 2.2. Assumptions made for the steam cycle for the design point are

summarised in Table 1. In Table 2 are given some essential performance parameters at design for the combined cycles featuring two-shaft and single-shaft gas turbines, respectively. The minor differences in performance between the single and two-shaft configurations are a consequence of the gear loss (which is assumed to be 1% at design) for the cycle with single-shaft gas turbine configuration (see Haglind [30]).

4. Part-load performance

The output of the combined cycle is controlled by means of the gas turbines only. Then, the steam turbine will generate power with whatever steam is available from the HRSGs. It is assumed that the gas turbines are connected to generators rotating with constant speeds. This means that the rotational speed is constant for the single-shaft machine over the whole load range. For the two-shaft gas turbine, the speed of the gas generator is reduced, while the speed of the power turbine (which is connected to the power turbine) is constant in part-load. When using variable geometry, the exhaust temperature is kept constant to the extent possible in part-load.

As for the combined cycle with single-shaft gas turbine configurations, regular fuel flow load control is compared with VGV control. In the case of fuel flow control, the load is controlled purely by adjusting the fuel flow. The variable guide vane control implies that the VGVs are closed, while the fuel flow rate is reduced simultaneously for keeping the exhaust gas temperature constant. Considering the capabilities of modern compressors, it is assumed that inlet mass flow rate can be reduced by 40% using the VGVs. Subsequently, the VGV angle is kept constant while the fuel flow rate is lowered further, causing the exhaust temperature to decrease. Following this strategy the load can be reduced down to about 35% using the VGVs. In the case of

the combined cycle with two-shaft gas turbine configurations, fuel control as well as VAN control is applied. Considering what is attainable for the WR-21 engine (see Haglind [30]), 30% is considered the maximum possible reduction in power turbine non-dimensional flow using the VAN. This reduction is sufficient for decreasing the load down to 30%, enabling the exhaust temperature to be constant over the whole load range considered here.

The thermal efficiency versus load for the load range 30-100% (corresponding approximately to 40-100% combined cycle load) are shown in Fig. 2 for the single-shaft and two-shaft gas turbine configurations employing fuel flow and variable geometry load control strategies, respectively. As is discussed in Haglind [30], the relative thermal efficiency in part-load is superior for the two-shaft arrangement. Moreover, the results for the gas turbines suggest that VGV control enables slightly increased thermal efficiency compared with fuel flow control at high powers, but for low powers the thermal efficiency is decreased, mainly as a consequence of the increasing detrimental effect on the compressor isentropic efficiency of the VGVs. The use of VAN control seems to reduce the efficiency over the whole load range compared with fuel flow control. Considering all the four curves, the two-shaft configuration using fuel flow control is indicated as giving the best gas turbine part-load performance.

As far as combined cycles featuring HRSGs of drum-type are concerned, in order to maximise the part-load efficiency, these are often operated in sliding pressure mode. That is, as the load is lowered, the live steam pressure is allowed to go down to the pressure corresponding to the swallowing capacity of the steam turbine. The pressure

can be lowered down to about 50% of the design pressure; below that point, the live steam pressure is held constant by closing the steam turbine control valves, resulting in throttle losses [11].

If the gas turbine is controlled such that the exhaust temperature is maintained in part-load, the live steam temperature can also be kept constant in part-load, which is beneficial for the efficiency of the Rankine cycle. Pinch- and approach points within the HRSG are defined at design, and in part-load the magnitudes of these are governed by the heat transfer coefficients within the heat exchangers. As a consequence, as the load is reduced with constant gas turbine exhaust temperature, the live steam temperature would increase. Increased live steam temperature is, however, not acceptable because of the increased thermal load on the steam turbine. This problem can be resolved by attemperation after the superheater. That is, feedwater (normally from the high-pressure circuit) is injected into the live steam to cool it down to the required temperature. In general, attemperation is used in combined cycles to reduce the temperature peaks during off-design operating conditions, such as hot ambient temperatures, part-load and peak-load [11].

One thing that needs to be considered, especially when designing combined cycles for ship propulsion, is that combined cycles with HRSG design pressures of 100 bar and beyond are restricted with respect to their ability to respond to sudden load changes when operated in sliding pressure mode. This is because of the thermal stresses on the drum caused by the varied pressure. Moreover, the start-up and shut-down times are affected detrimentally by sliding pressure mode operation. For improving these operational constraints, the steam turbine control valves can be used to retain the

drum pressure in part-load. However, that would give rise to throttle losses that would decrease the plant efficiency.

In this study the pressure is significantly lower than 100 bar, thus sliding-pressure mode is believed to be a suitable control method. When applying load control methods for which the gas turbine exhaust temperature is retained, attemperation is used to limit the live steam temperature (see Fig. 1). Also shown in Fig. 1 is a steam turbine by-pass. This is used to provide flexible operation (e.g. during start-up, shut-down and quick load changes) and to reduce the start-up time. As described in Section 3.2, the steam produced in the low-pressure evaporator is used for feedwater pre-heating and for generating additional power in the steam turbine. When running in part-load, the division between the feedwater tank and steam turbine is adjusted to meet the requirement for feedwater pre-heating. For all the cases studied here the low-pressure steam is sufficient for feedwater pre-heating over the whole load ranges.

Relative net steam cycle power output versus gas turbine load is depicted in Fig. 3 and the combined cycle thermal efficiency versus combined cycle load is depicted in Fig. 4. In Fig. 3 are included the gas turbine load ranges corresponding to the load ranges 40-100% for the combined cycles. The load of the gas turbines is in all cases lowered equally and simultaneously. The part-load characteristics of the combined cycle featuring the single-shaft gas turbines with VGV control (shown in Fig. 4) agree well with those of corresponding stationary combined cycles [11]. This comparison suggests that the combined cycle performance results are reasonable. However, due to the lack of detailed manufacturer/experimental data with respect to the variable area nozzle turbine performance (see Haglind [30]), the results for the cycle with two-shaft

gas turbine using VAN control are associated with the larger uncertainties than the others.

The beneficial effect on the steam cycle performance of maintaining the gas turbine exhaust temperature in part-load using variable geometry is illustrated in Fig. 3. For both the combined cycles with single- and two-shaft gas turbines, the results suggest that the drop in steam turbine power output with reduction in load is significantly lower when employing variable geometry. Between 80% and 100% load, the cycle with two-shaft gas turbine using VAN control achieves the best steam turbine performance, and for lighter loads, the cycle with single-shaft gas turbine using VGV control attains the best steam turbine performance.

As for the combined cycles, between 80% and 100% loads, the results suggest that the cycle featuring single-shaft gas turbines using VGV control gives the highest efficiency in part-load. Below that point the cycle with two-shaft gas turbines using VAN control is indicated as having the highest efficiency. This behaviour is determined by characteristics of the gas turbines and the steam cycle, as expressed in Eq. (1) (see Figs. 2-3). Comparing these two cases employing variable geometry, between 80% and 100% the penalty in gas turbine efficiency is smaller for the single-shaft arrangement, but below 80% load the gas turbine efficiency drops off with a much higher rate for the single-shaft configuration. This behaviour is the opposite to that of the steam cycle power output, but, when it comes to the combined cycle performance, the results suggest that the effects of the gas turbine performance characteristics dominate.

Considering pure fuel flow control, the results indicate that the superior part-load performance for the two-shaft gas turbine compared with that of the singe-shaft configuration shown in Fig. 2 is even larger for combined cycles (see Fig. 4). This is to be expected, because, for a given load, the exhaust gas temperature drop is much smaller for a two-shaft gas turbine, resulting in a larger steam turbine output (see Fig. 3). The beneficial effect on the steam cycle plays a larger role the lighter the load, because of the increasing power contribution from the steam cycle with decreasing load. In general, for full power operation, the gas turbine(s) accounts for about two-thirds of the power output and the steam turbine for one-third, while this ratio is reversed at about 20% combined cycle load, with the steam turbine contributing two-thirds of the power output and the gas turbine one-third [11]. The cycle with the single-shaft configuration using fuel flow control is the option that offers the worst part-load performance. This is expected because the exhaust gas turbine temperature drops off with a much higher rate in this case than in the others.

A further option for improving the part-load performance of combined cycles including more than one gas turbine which is not addressed here is to control the gas turbines differently when reducing the load. By lowering the load to a minimum for each gas turbine before the load is reduced for the next gas turbine, a previous study [43] and experience with the Millennium cruise ship [44] have indicated that not negligible benefits in part-load performance can be obtained compared with those of reducing the load of the gas turbines similarly and simultaneously. Other design features that might have a beneficial effect on the combined cycle part-load performance include the use of reheat gas turbines [45] and supplementary firing in

the HRSG [43]. While the reheat gas turbines tend to increase also the design point performance, supplementary firing in the HRSG tends to decrease it.

5. Ship voyage performance

The combined cycles investigated can be evaluated with respect to voyage performance by considering some typical voyage load profiles for large ship types. As mentioned in Section 1, the largest container ships require propulsion powers of the magnitudes produced by the combined cycles considered here. Other large ships like bulk carriers and tankers require significantly lower powers, mainly because they are sailing with essentially lower speeds.

In order to meet the power requirements of bulk carriers and tankers, the combined cycles need to be scaled down or re-designed with only one or two smaller gas turbines. These are changes that will decrease the design point (as well as the part-load) performance. However, this paper is aimed at looking into methodologies for improving the part-load performance rather than designing advanced cycles for which very high efficiencies are attained. Therefore, the results are relevant also for bulk carriers and tankers, but one should be aware that for the same combined cycle design, lower efficiency figures than those presented here would be expected.

The load profile for a specific ship type is not fixed, but dependent on a range of factors, for instance, the demand for transportation, fuel prices, where the ship is sailing, and the actual voyage route plan (KR. Jensen, FORCE Technology, Denmark, 2008, private communication). When there is a high demand, the vessels are sailing as fast as possible in order to perform as many routes as possible, whereas the ships are

slowed down for saving fuel when the demand is low. High fuel prices is another incentive for ship owners to reduce the average sailing speed, and thereby save fuel costs. In general, container ships are sailing with a lower average load than tankers and carriers. This is because container ships often have a fixed schedule including margins for being able to handle congestion in ports.

In Fig. 5 typical voyage load profiles, which are selected on the basis of ship owners' experience, for container ships, and tankers and carriers are shown (KR. Jensen, FORCE Technology, Denmark, 2008, private communication). In the figure, 100% load corresponds to the service continuous rating (SCR), which is the maximum engine power used in service. In this case SCR is assumed to be 85% of the maximum power that a diesel engine would be able to produce, which is called the maximum continuous rating (MCR). The 15% margin includes a so-called sea margin for being able to handle fouled hull and propeller (causing increasing resistance), and heavy weather. In addition, the margin includes an engine margin to ensure that the diesel engine is not running at its maximum power (for durability and maintenance reasons).

A gas and steam turbine combined cycle used for ship propulsion should be operated as close as possible to the maximum power as much as possible of the time, because it is in this operating point the combined cycle achieves its highest efficiency. This is in contrast to marine slow-speed diesel engines for which the efficiency generally is maximum at about 80% load. When considering combined cycles for ship propulsion there is no reason to include an engine margin, but a capability for handling fouling and bad weather needs to be addressed in one way or another. For resolving this the combined cycle can be designed so that it is possible to run it with higher maximum

temperatures (i.e. turbine inlet temperature and live steam temperature) than in design for a limited time period, or reduced sailing speed due to fouling and/or bad weather is accepted. Another possibility, which would increase the investment cost of the prime mover system, is to install another gas turbine or diesel engine that may assist the combined cycle in such circumstances. Such additional machinery might also be useful for producing auxiliary power in port.

In this paper the combined cycles are evaluated based on the assumption that the 100% load in Fig. 5 corresponds to full load conditions for the combined cycles. Using the part-load performance figures shown in Fig. 4 and the voyage load profiles presented in Fig. 5, average relative voyage thermal efficiencies for the four different options are calculated; see Fig. 6. For container ships, the results suggest that a combined cycle featuring two-shaft gas turbines with VAN control is a promising alternative for minimising the voyage fuel consumption. For ships sailing at a higher average rating, like tankers and carriers, a combined cycle with single-shaft gas turbine configurations with VGV control is indicated to be an equally good choice.

6. Conclusions and discussion

In this paper combined cycles for marine applications, with and without variable geometry gas turbines, have been designed and their performances have been estimated. In addition, methodologies have been developed and models have been derived for part-load modelling of HRSGs and steam turbines.

Considering pure fuel flow control, the results indicate that the superior part-load performance for the two-shaft gas turbine compared with that of the single-shaft

configuration is even greater for combined cycles. Moreover, the results suggest that by the use of variable geometry gas turbines, the combined cycle part-load performance can be improved. For loads between 80% and 100%, the results suggest that the cycle featuring single-shaft gas turbines using VGV control gives the best part-load performance. Below that point the cycle with two-shaft gas turbines using VAN control is indicated to have the highest efficiency.

In order to minimise the voyage fuel consumption for container ships, the results suggest that a combined cycle featuring two-shaft gas turbines with VAN control is a promising alternative. For ships typically sailing at a higher average rating, like tankers and carriers, a combined cycle with single-shaft gas turbine configurations with VGV control is indicated to be an equally good choice. Considering container ships (for which combined cycles are believed to be the most suitable), the improvement in average (relative) voyage thermal efficiency of using variable geometry gas turbines is 3.1% for the cycle with single-shaft configurations, and 0.9% for the cycle with two-shaft configurations. It needs to be emphasised that given that the differences in performance among the different cases are small and that the results are based on a number of assumptions associated with uncertainties, the results should be interpreted with caution.

Acknowledgements

The work has greatly benefited from discussions with my colleague Brian Elmegaard (from the same institute), who has also contributed to the implementation of models for part-load simulation of gas turbines in DNA. Jari Nyqvist, Siemens Industrial Turbomachinery, Finnspång, Sweden, is thanked for having provided information on

the SST-300 steam turbine, and Kjeld Roar Jensen at FORCE Technology, Denmark, is thanked for having provided information on ship voyage load profiles. The funding from the Danish Center for Maritime Technology (DCMT) is acknowledged.

References

[1] V. Eyringer, H.W. Köhler, A. Lauer, B. Lemper, Emissions from international shipping: 2. Impact of future technologies on scenarios until 2050, J Geophys Res 110 (2005), D17306.

[2] F. Haglind, A review on the use of gas and steam turbine combined cycles as prime movers for large ships, Part I: Background and design, Energy Convers. Manage. 49 (12) (2008) 3458-3467.

[3] F. Haglind, A review on the use of gas and steam turbine combined cycles as prime movers for large ships, Part II: Previous work and implications, Energy Convers. Manage. 49 (12) (2008) 3468-3475.

[4] F. Haglind, A review on the use of gas and steam turbine combined cycles as prime movers for large ships, Part III: Fuels and emissions, Energy Convers. Manage. 49 (12) (2008) 3476-3482.

[5] J.H. Kim, T.S. Kim, J.L. Sohn, S.T. Ro, Comparative Analysis of Off-Design Performance Characteristics of Single and Two-Shaft Industrial Gas Turbines, J. Eng. Gas Turbines Power 125 (2003) 954-960.

[6] T.S. Kim, T.S. Ro, The effect of gas turbine coolant modulation on the part load performance of combined cycle plants Part 1: gas turbines, Proc Instn Mech Engrs Vol 211 Part A (1997) 443-451.

[7] T.S. Kim, T.S. Ro, The effect of gas turbine coolant modulation on the part load performance of combined cycle plants Part 2: combined cycle plant, Proc Instn Mech Engrs Vol 211 Part A (1997) 453-459.

[8] P.J. Dechamps, N. Pirard, Ph. Mathieu, Part-Load Operation of Combined Cycle Plants With and Without Supplementary Firing, J. Eng. Gas Turbines Power 117 (1995) 475-483.

[9] U. Desideri, A. Fibbi, A Simplified Approach to Off-Design Performance Evaluation of Combined Cycle Powerplants with Single-Pressure Steam Cycles, in: IGTI Vol. 8, ASME COGEN-TURBO, 1993, pp. 199-207.

[10] W.I. Rowen, R.L. Van Housen, Gas Turbine Airflow Control for Optimum Heat Recovery, J. Eng. Gas Turbines Power 105 (1983) 72-79.

[11] R.H. Kehlhofer, J. Warner, H. Nielsen, R. Bachmann, Combined-Cycle Gas & Steam Turbine Power Plants, 2nd ed., PennWell, Tulsa, Oklahoma, 1999.

[12] P.P. Walsh, P. Fletcher, Gas Turbine Performance, Blackwell Science Ltd, Malden, 1998.

[13] T.S. Kim, S.H. Hwang, Part load performance analysis of recuperated gas turbines considering engine configuration and operation strategy, Energy 31 (2006) 260-277.

[14] J.C. Cox, D. Huthinson, J.I. Oswald, The Westinghouse/Rolls-Royce WR-21 Gas Turbine Variable Area Power Turbine, ASME paper GT-95-54, 1995.

[15] W. Stossier, M. Stauffer, G.E. Perkins, WR-21 Recuperator Core Test, in: Proceedings of the International Gas Turbine and Aeroengine Congress and Exhibition, 2-5 June, Orlando, Florida, USA, 1997.

[16] C.L. Weiler, A. Broadbelt, B. Law, WR-21 Design and Maintenance, in: Proceedings of the International Gas Turbine and Aeroengine Congress and Exhibition, 10-13 June, Birmingham, UK, 1996.

[17] S.B. Shepard, T.L. Bowen, J.M. Chiprich, Design and Development of the WR-21 Intercooled Recuperated (ICR) Marine Gas Turbine, J. Eng. Gas Turbines Power 117 (1995) 557-562.

[18] R.L. Kiang, T.L. Bowen, Application of Advanced heat Exchanger Technology in a 22MW Naval Propulsion Gas Turbine, in: Proceedings of ASME/JSME Thermal Engineering Conference Vol. 4, 1995. pp. 347-358.

[19] R.P. North, R.E. Dawson, The Design and Initial Development of a Combustion System for the WR-21 Intercooled Recuperated Gas Turbine, in: Proceedings of the International Gas Turbine and Aeroengine Congress and Exhibition, 5-8 June, Houston, Texas, USA, 1995.

[20] A.J. Crisalli, M.L. Parker, Overview of the WR-21 Intercooled Recuperated Gas Turbine Engine System A Modern Engine for a Modern Fleet, in: Proceedings of International Gas Turbine and Aeroengine Congress and Exhibition, 24-27 May, Cincinnati, Ohio, USA, 1993.

[21] C. Bringhenti, J.R. Barbosa, Part-Load versus Downrated Industrial Gas Turbine Performance, in: Proceedings of ASME Turbo Expo 2004, Vienna, Austria, Vol. 7. 2004. pp. 633-639.

[22] C. Bringhenti, J.R. Barbosa, Study of an Industrial Gas Turbine with Turbine Stators Variable Geometry, in: Proceedings of 9th Brazilian Congress of Thermal Engineering and Sciences, Caxambu – MG, Brazil, paper CIT02-0885.

[23] C. Bringhenti, J.R. Barbosa, Effects of Variable-Area Turbine Nozzle over the Important Parameters of gas Turbine Performance, in: Proceedings of II National Congress of Mechanical Engineering 2002, João Pessoa PB, Brazil.

[24] J.E.A. Roy-Aikins, A Study of Variable Geometry in Advanced Gas Turbines, Ph.D. thesis, Cranfield Institute of Technology, UK, 1988.

[25] A.L. Polyzakis, C. Koroneos, G. Xydis, Optimum gas turbine cycle for combined cycle power plant, Energy Convers. Manage. 49 (2008) 551-563.

[26] O. Bolland, A Comparative Evaluation of Advanced Combined Cycle Alternatives, ASME paper 90-GT-335, 1990.

[27] Propulsion Trends in Container Vessels, MAN B&W Two-stroke Engines. MAN Diesel A/S, Copenhagen, Denmark, http://www.mandiesel.com/files/news/filesof4672/Propulsion_trends_in_container_vessels.pdf, downloaded 2009.

[28] Propulsion Trends in Bulk Carriers. MAN Diesel A/S, Copenhagen, Denmark, http://www.mandiesel.com/files/news/filesof5479/5510-0007-01ppr.pdf, downloaded 2009.

[29] Propulsion Trends in Tankers. MAN Diesel A/S, Copenhagen, Denmark, http://www.mandiesel.com/files/news/filesof8073/5510-0031-00.pdf, downloaded 2009.

[30] F. Haglind, Variable geometry gas turbines for improving the part-load performance of marine combined cycles – Gas turbine performance, Energy 35 (2010) 562-570.

[31] B. Elmegaard, N. Houbak, DNA – A General Energy System Simulation Tool, in: Proceedings of SIMS 2005, Trondheim, Norway, 2005.

[32] B. Elmegaard, Simulation of Boiler Dynamics – Development, Evaluation and Application of General Energy System Simulation Tool. Ph.D. thesis, Technical University of Denmark, Denmark, 1999.

[33] C. Perstrup, Analysis of power plant installation based on network theory (in Danish). M.Sc. thesis, Technical University of Denmark, Denmark, 1991.

[34] F. Haglind, B. Elmegaard, Methodologies for predicting the part-load performance of aero-derivative gas turbines. Energy 34 (2009) 1484-1492.

[35] O. Bolland, Thermal Power Cycles and Cogeneration, Lecture Notes, EP8103, Norwegian University of Science and Technology, Trondheim, Norway, 2003.

[36] W.M. Kays, A.L. London, Compact Heat Exchangers, Third Edition, McGraw-Hill Book Company, New York, 1984.

[37] M. De Salve, M. Malandrone, G. Pedrelli, A. Scerrati, G. Scorta, A Model for Thermal-Hydraulic Analysis of Heat Recovery Steam Generators (HRSG) for Combined-Cycle Plants. An Application to Comparison of Different HRSG Sizings, in: Proceedings of the 10th International Heat Transfer Conference, Brighton, UK, 1984.

[38] D.H. Cooke, On Prediction of Off-Design Multistage Turbine Pressures by Stodola's Ellipse, J. Eng. Gas Turbines Power 107 (1985) 596-606.

[39] G.T. Csanady, Theory of Turbomachines, McGraw-Hill, New York, 1964.

[40] R.C. Spencer, K.C. Cotton, C.N. Cannon, A method for Predicting the Performance of Steam Turbine-Generators…16,500 kW and Larger, J. Eng. Gas Turbines Power October (1963) 249-301.

[41] K.C. Cotton, Evaluating and Improving Steam Turbine Performance, 2nd Edition, Cotton Fact Inc., New York, 1998.

[42] S.C. Stultz, J.B. Kitto, Steam, its generation and use, fortieth edition, The Babcock & Wilcox Company a McDermott company, Barberton, USA 1992.

[43] P.J. Dechamps, N. Pirard, Ph. Mathieu, Part-Load Operation of Combined Cycle Plants With and Without Supplementary Firing, J. Eng. Gas Turbines Power 117 (1995) 475-483.

[44] B.N. Sannemann, Pioneering Gas Turbine-Electric System in Cruise Ships: A Performance Update, Marine Technology 41 (2004) 161-166.

[45] H.I.H. Saravanamuttoo, G.F.C Rogers, H. Cohen, P.V. Straznicky, Gas Turbine Theory, 6th Edition, Pearson Education Limited, Harlow, UK, 2009.

Fig. 1. Schematic figure of the combined cycle.

Fig. 2. Relative gas turbine thermal efficiency versus gas turbine load.

Fig. 3. Relative net steam cycle output versus gas turbine load.

Fig. 4. Relative combined cycle thermal efficiency versus combined cycle load.

Fig. 5. Typical voyage load profiles for container ships and tankers/carriers.

Fig. 6. Average relative voyage thermal efficiency for container ship and tanker/carrier.

Table 1

Assumptions for the steam cycle at design.

Efficiencies	
Pump efficiency [%]	80
Steam turbine isentropic efficiency [%]	87
Steam turbine mechanical/steam turbine generator efficiency [%]	97.5
HRSG conditions	
Pinch-point [ºC]	10
Superheater approach [ºC]	30
Economiser approach [ºC]	5-100
Pressure loss, gas side [mbar]	30
Pressure loss, water/steam side [bar]	6.667
Steam turbine conditions	
Live steam temperature [ºC]	506.8
Live steam pressure [bar]	60
Other steam cycle conditions	
Dearator pressure [bar]	1.17
Feedwater temperature [ºC]	104
Condensor pressure [bar]	0.035

Table 2

Combined cycle performances at design.

	1-shaft gas turbine	2-shaft gas turbine
Gas turbine exhaust temperature [°C]	536.5	536.8
Total gas turbine power output [MW]	60.86	61.43
High-pressure steam mass flow [kg/s]	22.22	22.23
Low-pressure steam mass flow [kg/s]	3.31	3.30
Net steam cycle power output [MW]	27.56	27.57
Combined cycle power output [MW]	88.42	89.00
Combined cycle thermal efficiency [%]	53.48	53.83

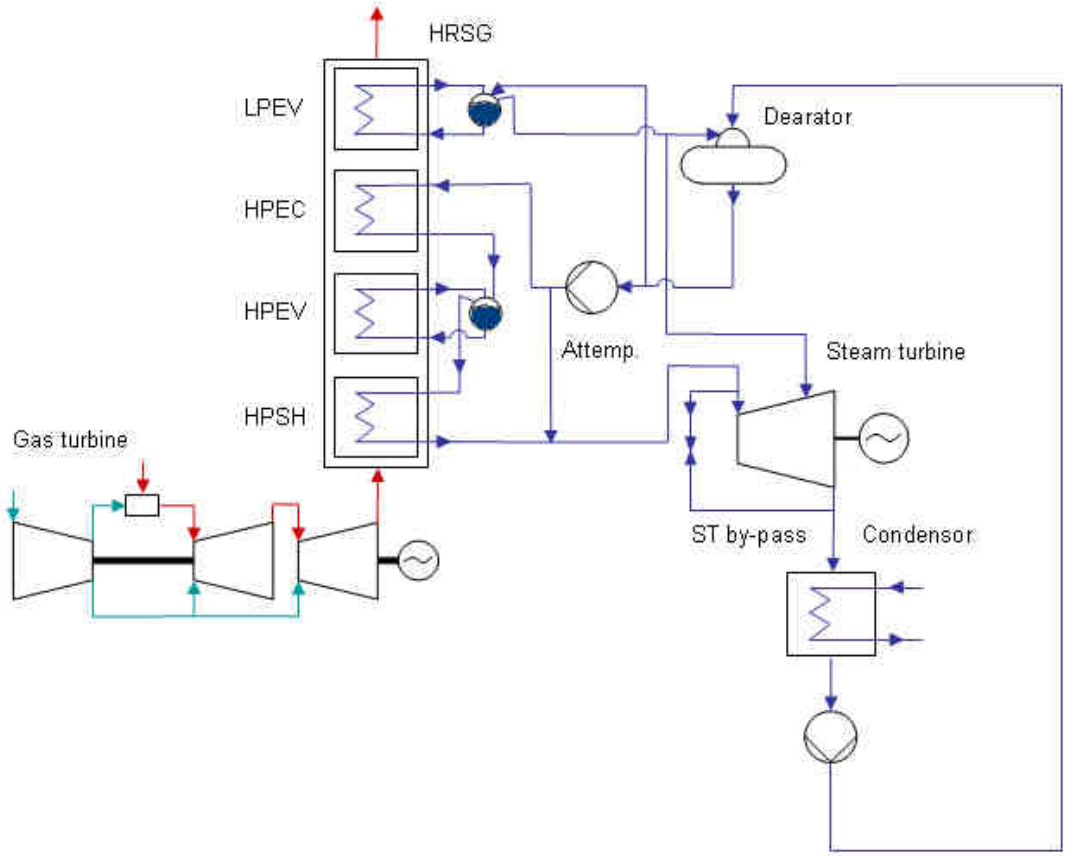

Fig. 1. Schematic figure of the combined cycle.

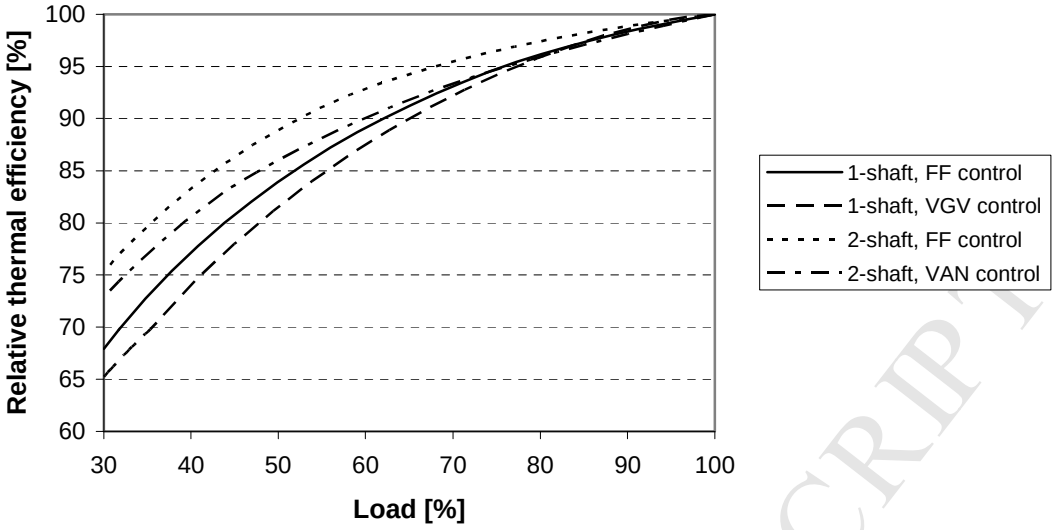

Fig. 2. Relative gas turbine thermal efficiency versus gas turbine load.

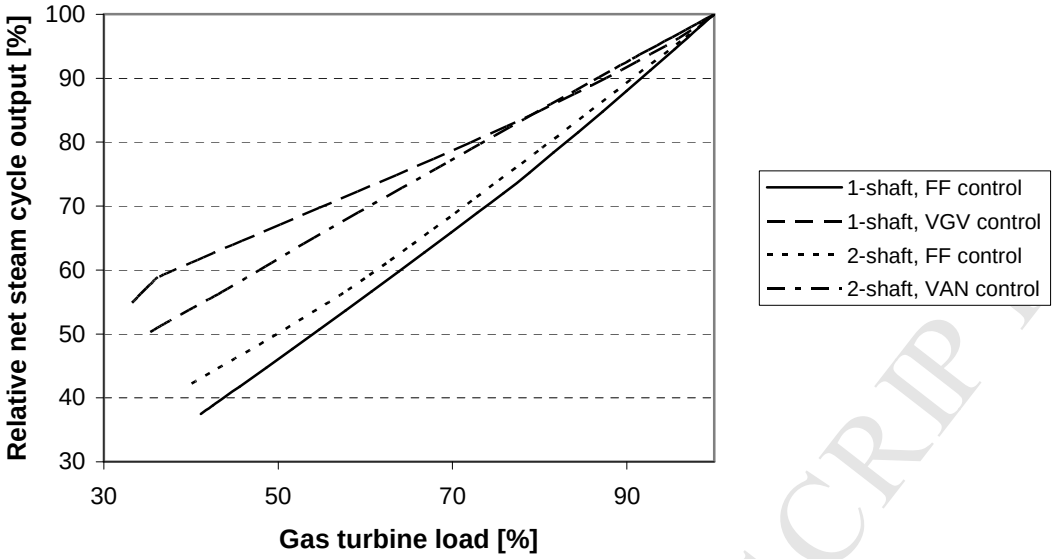

Fig. 3. Relative net steam cycle output versus gas turbine load.

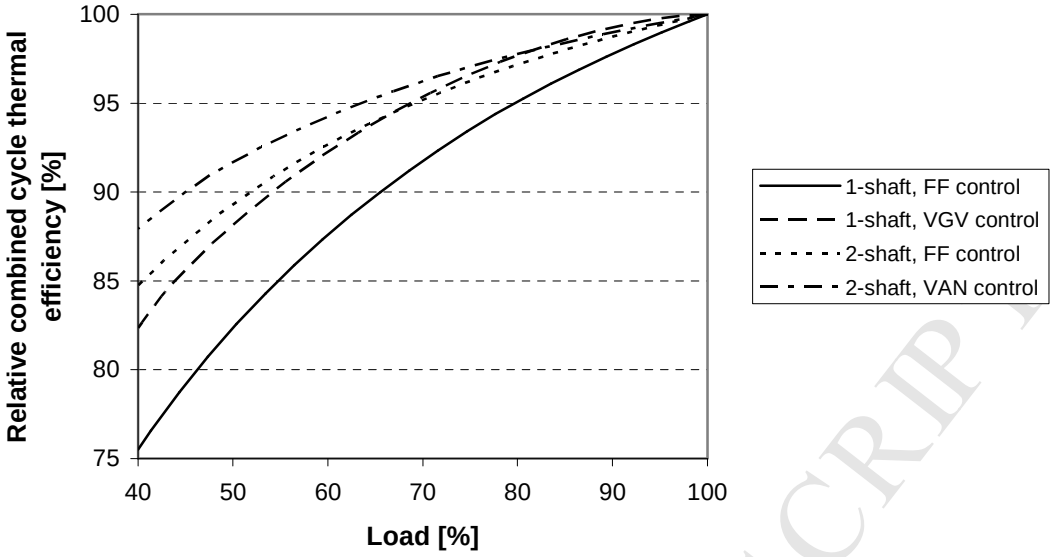

Fig. 4. Relative combined cycle thermal efficiency versus combined cycle load.

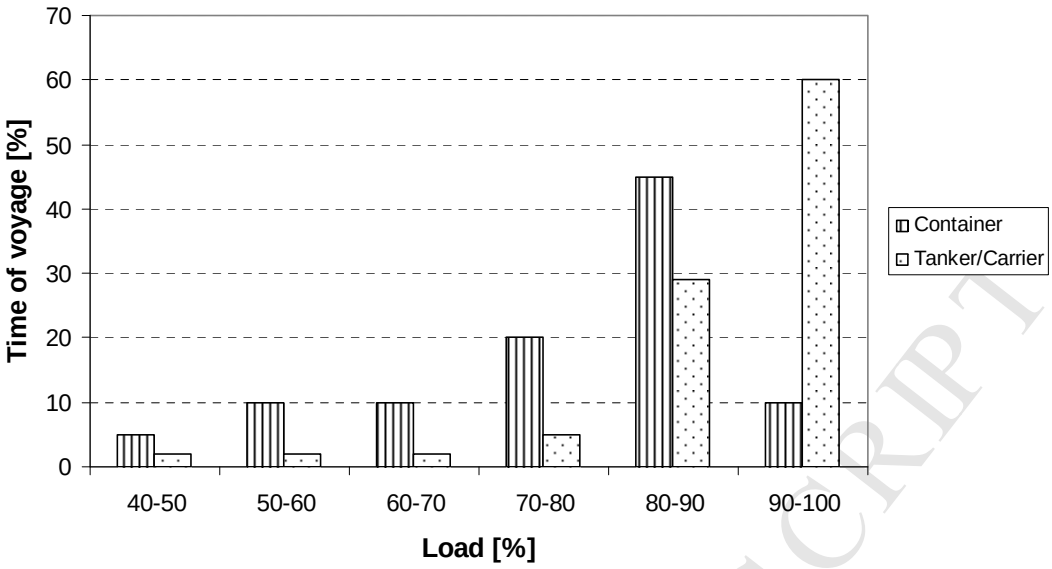

Fig. 5. Typical voyage load profiles for container ships and tankers/carriers.

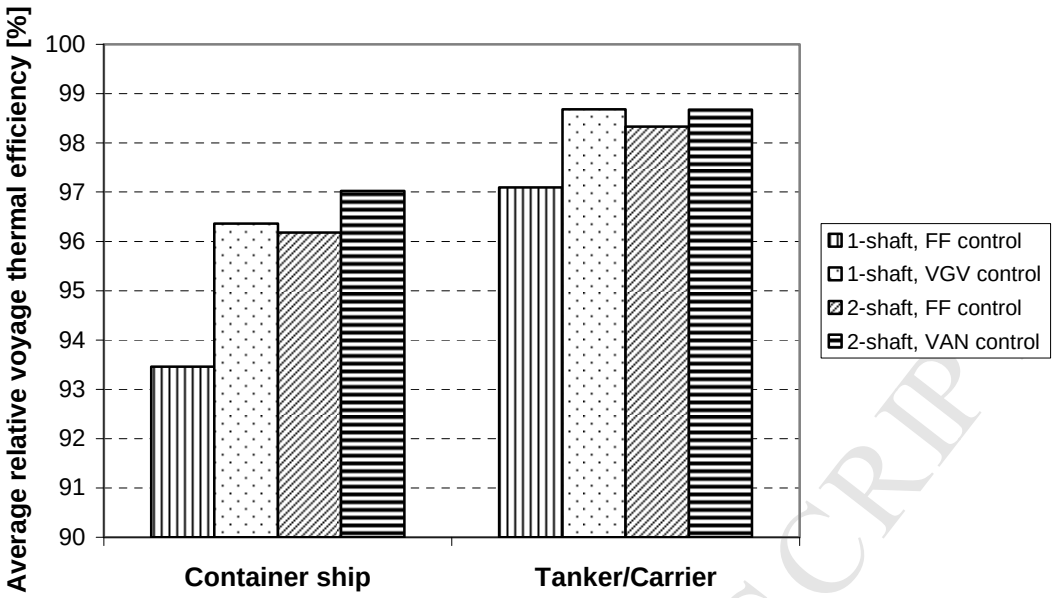

Fig. 6. Average relative voyage thermal efficiency for container ship and tanker/carrier.